

LYNX: ENABLING EFFICIENT MOE INFERENCE THROUGH DYNAMIC BATCH-AWARE EXPERT SELECTION

Vima Gupta¹ Kartik Sinha¹ Ada Gavrilovska¹ Anand Padmanabha Iyer¹

ABSTRACT

Mixture-of-Experts (MoE) architectures have recently gained popularity in enabling efficient scaling of large language models. However, we uncover a fundamental tension: while MoEs are designed for selective expert activation, production serving requires request batching, which forces the activation of all experts and negates MoE’s efficiency benefits during the decode phase. We present LYNX, a system that enables efficient MoE inference through dynamic, batch-aware expert selection. Our key insight is that expert importance varies significantly across tokens and inference phases, creating opportunities for runtime optimization. LYNX leverages this insight through a lightweight framework that dynamically reduces active experts while preserving model accuracy. Our evaluations show that LYNX achieves up to $1.55\times$ reduction in inference latency while maintaining negligible accuracy loss from baseline model across complex code generation and mathematical reasoning tasks.

1 INTRODUCTION

Large Language Models (LLMs) have achieved phenomenal breakthroughs in difficult tasks like solving mathematical problems and code generation, exceeding human expectations heralded by training on high quality data and increasing the number of model parameters (Naveed et al., 2023; Luo et al., 2024; Yin et al., 2024). The trend toward increasingly larger models shows no sign of abating, making scaling an inevitable aspect of developing more powerful LLMs (Kaplan et al., 2020; Yun et al., 2024).

The *Mixture-of-Experts (MoE)* architecture has emerged as a promising approach to efficient scaling. MoEs build on a key insight: not all inputs require the full computational capacity of a large model. By decomposing the network into specialized experts that handle distinct aspects of the input, MoEs enable selective computation where only a subset of parameters is activated for each input. This approach has enabled models to scale beyond hundreds of billions of parameters while maintaining reasonable computational costs during training.

Real-world deployment reveals a critical paradox in MoE design. Consider what happens in production: a language service like ChatGPT (OpenAI, 2024) and Claude (Anthropic, 2024) processes millions of requests concurrently. To handle this load efficiently, the service must batch multiple requests together (Kwon et al., 2023; Yu & Jeong, 2022;

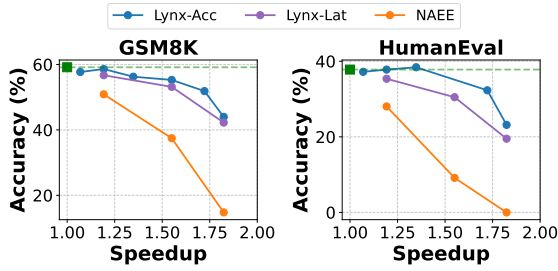


Figure 1: LYNX achieves superior latency-accuracy trade-offs compared to static pruning (NAEE) across complex tasks. On GSM8K, LYNX maintains over 55% accuracy even at 1.5x speedup while NAEE drops below 40%. The gap is even more pronounced for HumanEval, where LYNX retains over 30% accuracy at 1.75x speedup while NAEE’s accuracy collapses. This demonstrates that dynamic expert selection based on runtime information significantly outperforms static approaches.

Agrawal et al., 2024). The fundamental problem emerges in how these batched requests interact – each request in the batch wants different experts. In a typical MoE where each input activates just two out of eight experts, a batch of four diverse requests is enough to activate every expert in the model. The promise of MoEs, that we only pay for the experts we use, breaks down completely. Instead of getting the efficiency of selective computation, we end up paying the full cost of loading all model parameters from memory, exactly what MoE designs tried to avoid.

The challenge is particularly acute during the decode phase, where memory bandwidth dominates latency (Yun et al.,

¹Georgia Institute of Technology, USA. Correspondence to: Vima Gupta <vima.gupta@gatech.edu>.

2024). While the prefill phase can hide memory access costs through parallel computation, token generation remains fundamentally memory-bound. Even when models fit in GPU memory, latency-critical applications struggle with modest batch sizes due to the overhead of moving parameters from high-bandwidth memory to streaming multiprocessors. Understanding and resolving this tension between batching and selective computation is crucial for realizing the promise of MoE architectures at scale.

The difficulty of optimizing MoE computation stems from how experts specialize during training. MoEs employ load balancing to ensure uniform expert utilization, leading to balanced expert activation patterns across tasks. Prior approaches have explored expert reduction during pre-training (Do et al., 2023; Chen et al., 2023) and runtime (Lu et al., 2024), but face fundamental limitations. Static expert reduction through pruning (Lu et al., 2024) or merging (Li et al., 2023) requires prior knowledge of downstream tasks, making it impractical for general-purpose serving systems. Meanwhile, reducing the number of experts selected per token (top_k) proves ineffective - batch serving still activates the full expert pool while compromising model quality. Figure 1 illustrates this trade-off between computation and accuracy - existing approaches that reduce expert computation show significant accuracy degradation on complex tasks like GSM8k (Cobbe et al., 2021) and HumanEval (Chen et al., 2021). This creates a critical challenge for production systems that must maintain both serving efficiency and model capability.

In this paper, we present LYNX, a system that significantly reduces MoE inference latency while maintaining model accuracy. LYNX operates at batch granularity, dynamically optimizing expert computation for each layer based on runtime information. The system requires no model modifications or task-specific tuning, making it immediately applicable to existing MoE deployments.

LYNX’s design builds on three fundamental properties we discovered in MoE inference. First, the router network’s confidence scores prove highly predictive of which token-expert mappings are critical for model quality. Second, expert selection follows a clear hierarchy - primary expert choices contribute significantly more to output quality than secondary selections. Third, the impact of expert selection varies markedly between inference phases, with prefill showing high sensitivity while decode demonstrates substantial resilience. These properties reveal specific opportunities for optimization: LYNX leverages router confidence to identify critical tokens, prioritizes primary expert selections, and applies more aggressive optimizations during decode. By exploiting these patterns, LYNX dynamically adapts expert computation using only runtime information, maintaining model quality while significantly reducing serving costs.

Here are the key contributions of our work.

- We identify a key challenge in MoE serving, namely, how the promise of selective activation is negated in batched inference.
- LYNX leverages inherent heterogeneity in fundamental properties of MoE inference: router confidence predicts critical tokens, expert selection follows a clear hierarchy, and expert assignment impact varies markedly across inference phases.
- LYNX enables runtime expert optimization using only router outputs, eliminating the need for task-specific calibration or workload prediction. The system adapts expert computation based on batch-specific patterns while preserving critical token-expert mappings.
- LYNX introduces a dynamic optimization framework for MoE computation that works at batch granularity, reducing serving latency by $1.55\times$ while maintaining negligible drop in model accuracy.

2 BACKGROUND

Large language models process input using two distinct phases: prefill and decode. During prefill, the model processes the input prompt in parallel, generating hidden states that capture the input context. The decode phase then generates output tokens one at a time, using these hidden states along with previously generated tokens. This auto-regressive generation means that decode iterations typically dominate serving costs in production deployments for generative tasks. As models grow larger, serving them efficiently becomes increasingly challenging. Dense architectures, where every input activates all model parameters, face prohibitive computational and memory costs at scale.

2.1 MoE Architecture and Serving

The key principle behind MoEs is selective computation: not all inputs require the full computational capacity of a large model. Rather than processing every input through the entire network as in dense transformers, MoEs use specialized sub-networks (experts) that are selectively activated based on input characteristics.

A router network examines each input token and directs it to the most relevant experts. The expert selection process follows a two-step approach. First, the router network computes logits for each expert, which are transformed into selection probabilities through softmax normalization:

$$p_i = \frac{e^{z_i}}{\sum_{j=1}^N e^{z_j}} \quad (1)$$

where p_i represents the probability of selecting expert i , z_i is the router logit for expert i , and N is the to-

tal number of experts. The model then selects the k experts with highest routing probabilities: $E(x) = i \in 1, \dots, N : p_i$ is among top k values, where $E(x)$ represents the set of selected experts for input token x .

Modern LLM serving systems must process multiple requests simultaneously. Due to load-balancing loss function during training, different tokens in a batch tend to activate different experts. Even moderate batch sizes lead to the activation of all experts in the model. In Figure 3 (b), we vary the batch size from 1 to 32 and we observe that even for a batch size of 16, all experts end up getting activated. To understand whether our workload is compute-intensive or memory-intensive, we study the arithmetic intensity of MoE models as a function of the model parameters. It is a direct indicator of how well memory access costs can be hidden behind computation. The arithmetic intensity (operations per byte) during MoE inference exposes this fundamental challenge of memory boundedness of decode phase:

$$\text{Arithmetic Intensity} \approx \frac{n \cdot k}{\text{total_num_experts}} \quad (2)$$

Unlike dense models where operations amortize weight fetching across many tokens, MoE models suffer from reduced arithmetic intensity that scales inversely with expert count. Here k is the number of experts activated per token, total_num_exp shows the total number of experts per layer and n indicates the total number of tokens in the given batch. During prefill, the number of tokens is large enough to stay compute-bound while during batched decode, the number of tokens is much smaller. The decode phase becomes particularly memory-bound, as shown in Figure 3.

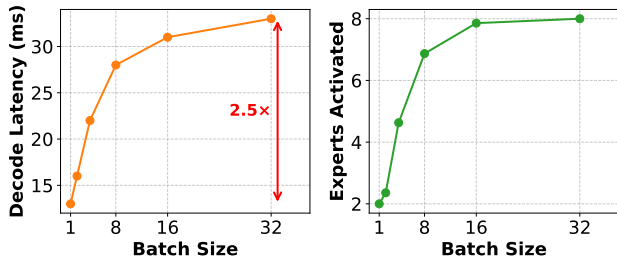


Figure 2: Impact of batching on decode latency. Even modest batch sizes (8-16) cause all experts to be activated, forcing each request to pay the memory access cost for the entire model. Left: Decode latency increases 2.5x as batch size grows from 1 to 32, demonstrating memory bandwidth bottleneck. Right: Number of activated experts rapidly saturates to maximum (8) with increasing batch size, showing how batching undermines MoE’s selective computation design.

In MoEs, the prefill phase continues to remain compute bound, while as the number of experts increase, decode phase becomes increasingly memory bound. While MoEs

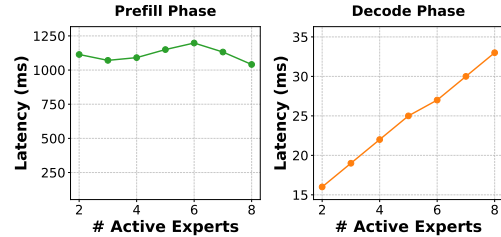


Figure 3: Prefill phase is compute-bound while decode is memory-bound. Left: Prefill latency remains relatively constant (~ 1000 ms) regardless of active experts, indicating compute-bound behavior. Right: Decode latency scales linearly with the number of active experts, revealing memory bandwidth as the bottleneck. This asymmetry in performance characteristics motivates phase-specific optimization strategies for MoE serving.

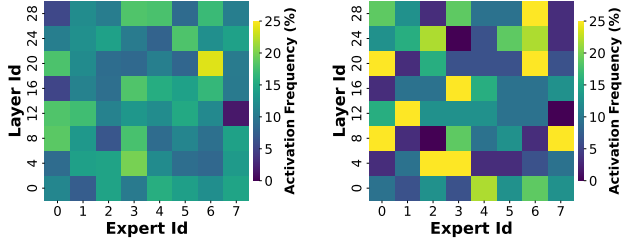
are designed for computational efficiency through selective activation, our analysis in Figure 3(a) shows that in batched serving scenarios, latency cost of MoEs is proportional to the model size and not the subset of experts activated for each token. This can be attributed to the memory-bound nature of decode phase where majority of the time is spent in fetching expert parameters from the memory. The end result is counter-intuitive - despite each token only using a few experts, every request ends up paying the memory access cost for the entire model during batched serving.

Takeaway 1: During the memory-bound decode phase, the latency in MoE’s scales with total number of expert parameters rather than activated parameters, rendering them inefficient at inference.

2.2 Expert Activation Patterns

Expert assignment for each token is determined at runtime by the router’s softmax probabilities. During training, auxiliary load balancing losses encourage uniform expert utilization. Our analysis of expert activation across millions of tokens from the ShareGPT-V3 dataset confirms this uniformity - when examined at scale, no expert stands out as consistently underutilized. (Lu et al., 2024; Jiang et al., 2024)

However, examining activation patterns at batch-level granularity tells a different story. For iteration-level scheduling, which is the norm in LLM inference systems (Kwon et al., 2023), the composition of input batches varies from one iteration to the next. This dynamic batch composition leads to significant variation in which experts are activated, even though the aggregate distribution remains uniform. The variability in expert activation is significantly higher at individual batch level as compared to the aggregate as shown in Figure 5.



(a) Expert activation patterns showing uniform distribution at aggregate level across dataset. (b) Expert activation patterns showing significant skew at batch-level granularity.

Figure 4: Expert activation patterns at different granularities: (a) aggregate level and (b) batch level. While expert utilization appears uniform ($\sim 10\text{-}20\%$ activation frequency) when analyzed across the entire dataset, individual batches show significant heterogeneity (0-25% range), revealing opportunities for dynamic optimization during serving.

Identifying permanently underutilized experts is quite challenging and requires prior knowledge of the workload. The strong batch-level skew in expert activation hints at the possibility of dynamic expert management during serving time to reduce decode latency.

Takeaway 2: Expert activation shows strong heterogeneity at batch-level despite being uniform at an aggregate level.

3 LYNX DESIGN INSIGHTS

Our analysis reveals a critical challenge in MoE serving: while selective expert activation provides significant computational advantages during the compute-bound prefill phase, this benefit is effectively nullified during decode where batching requirements force activation of the entire expert set. In order to reduce the final set of experts to which an input batch of tokens is mapped, we need to have a fundamental understanding of how expert selection contributes to the downstream accuracy at the token level, batch level, layer level and iteration level granularity. In this section we present our key insights into the importance of expert selection and underlying heterogeneity in MoE models.

3.1 Are all top- k experts equal?

To understand the true importance of different expert selections, we conducted a systematic study comparing the impact of denying access to primary versus secondary expert choices.

Figure 6 quantifies this hierarchy by showing the impact of reassigning experts on downstream accuracy. The results reveal a striking asymmetry: modifying primary expert assignments devastates model performance while changes to secondary expert selection cause minimal disruption. Most

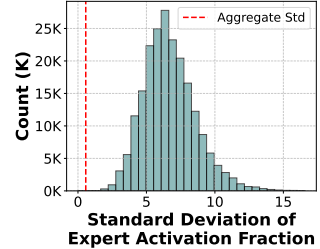


Figure 5: Expert activation patterns showing significant variability at batch-level granularity (standard deviation ranging from 0 – 15%) while at an aggregate level showcase much lower variability ($\sim 1.2\%$, red dashed line). This quantitative evidence of batch-level heterogeneity reveals opportunities for dynamic expert management during serving.

telling is the consistency of this pattern across different evaluation criteria - it reflects a fundamental property of how MoEs process information rather than an artifact of measurement.

This finding challenges our basic assumptions about MoE operation. The model doesn't actually need equal contribution from all selected experts - it relies heavily on primary selections while maintaining substantial redundancy in secondary choices. This variation in expert importance suggests that treating all expert computations equally during serving leaves significant optimization potential untapped.

Insight 1: The top ranking expert dominates output quality, with lower-ranked experts among $top-k$ showing high redundancy.

In LYNX, we leverage this insight of not all $top-k$ experts being equally important, to reduce the final set of activated experts for a given batch of tokens. Instead of retaining all $top-k$ experts, we prioritize retaining the primary expert while allowing for dropping of secondary experts.

3.2 Are all tokens equally important?

The router network in MoEs serves a critical role in matching tokens with appropriate experts. While most work treats router decisions as binary selections, our investigation reveals that the router's confidence in these selections carries crucial information about how different tokens interact with the expert pool.

To quantify this relationship, we analyzed how router confidence correlates with a token's sensitivity to expert reassignment. We developed a systematic way to measure router confidence and studied how tokens with different confidence levels respond to modifications in their expert assignments.

Figure 7 uncovers a fundamental pattern in this relationship. As we vary confidence thresholds, we observe a clear and growing separation between how high and low confidence

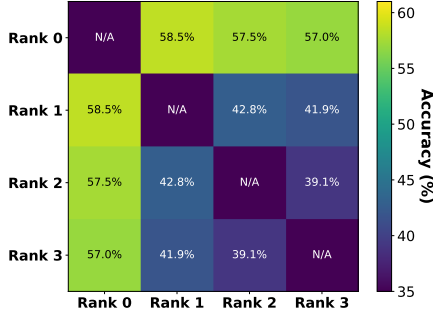


Figure 6: Expert selection hierarchy reveals optimization opportunities in MoE serving. Matrix shows accuracy impact when denying access to experts of different ranks. Denying rank-0 (primary) experts consistently degrades accuracy by 15-20 percentage points (vertical green column), while denying lower-ranked experts causes minimal impact (3-5 percentage point drops). This asymmetry enables efficient serving strategies that prioritize primary expert preservation while allowing flexible secondary expert assignment.

tokens respond to expert reassignment. High confidence tokens consistently demonstrate greater sensitivity to changes in expert assignment, while low confidence tokens show remarkable resilience. The diverging trends as confidence increases suggest we've identified a meaningful signal for distinguishing critical token-expert mappings from more flexible ones.

Just as not all experts contribute equally, not all tokens require the same level of computational precision. In LYNX, we extract ‘important’ tokens which are highly sensitive to expert reassignment and prioritize retaining their expert selection while allowing reassignment for the remainder of the tokens in the batch.

Insight 2: Router confidence provides a reliable signal for identifying critical token-expert mappings, to ensure expert reassignment has minimal impact on downstream accuracy.

3.3 Phase-specific Sensitivity

Perhaps our most surprising discovery concerns how MoE behavior varies across different phases of inference. The prevailing view treats expert selection as equally important throughout the inference process. Our investigation reveals this assumption significantly mischaracterize how MoEs actually process information.

To understand this phenomenon, we conducted a systematic comparison of how expert reassignment impacts model behavior during prefill versus decode phases. The experiment measured accuracy across different types of tasks, specifically chosen to stress different aspects of model capability.

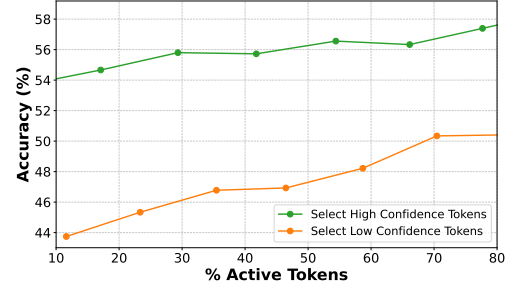


Figure 7: Relationship between router confidence and expert reassignment sensitivity. Low confidence tokens (orange line) maintain consistently higher accuracy under reassignment compared to high confidence tokens (green line). The growing separation with increasing confidence thresholds reveals fundamental differences in how tokens utilize expert computation.

Figure 8 reveals a striking asymmetry that persists across diverse workloads. Expert reassignment during prefill phase substantially impacts model performance on both code generation (HumanEval) and complex reasoning problems (GSM8K). In contrast, similar modifications during decode show minimal impact across all task types. This consistency across such different types of computation suggests we've uncovered a fundamental property of how MoEs process information rather than a task-specific phenomenon.

The explanation lies in the nature of autoregressive inference - the prefill phase establishes critical context that guides all subsequent computation, while the decode phase benefits from multiple mechanisms (attention, residual connections) that can compensate for suboptimal expert selection.

Insight 3: MoEs exhibit fundamentally different sensitivity to expert selection during prefill versus decode phases, enabling phase-specific optimization strategies.

These three properties - varying expert importance, token-level sensitivity, and phase-specific behavior - collectively point to the need for more nuanced serving strategies. The consistency of these patterns across different evaluation settings, tasks, and model scales suggests we've uncovered fundamental properties of MoE computation rather than implementation artifacts. This understanding reveals that efficient MoE serving requires adaptive decision-making that can respond to these variations at multiple scales. We detail our approach to this challenge in the next section.

4 DESIGN

4.1 System Overview

LYNX addresses a fundamental challenge in MoE serving: while selective expert activation is efficient during prefill,

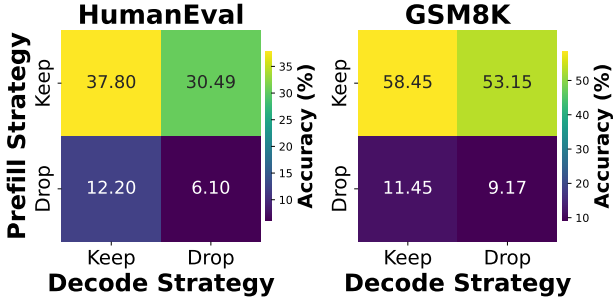


Figure 8: Phase-specific impact of expert reassignment across different task types. Code generation (HumanEval) and reasoning-heavy tasks (GSM8K) both show dramatic sensitivity during prefill but remarkable resilience during decode, revealing a fundamental asymmetry in how MoEs process information across phases.

batch serving typically forces full model activation during decode. Our design leverages the structured patterns we discovered in expert activation (Section 3) to maintain efficiency while preserving model quality.

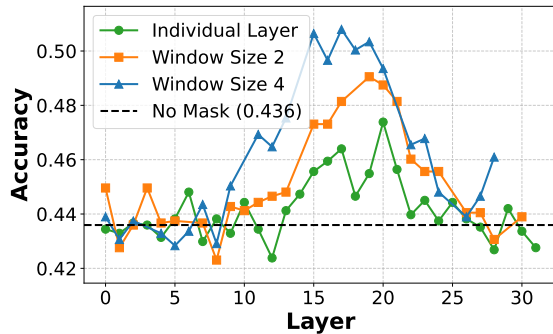


Figure 9: Layer-wise sensitivity analysis reveals opportunities for dynamic expert reduction. The graph shows accuracy impact when preserving expert assignments in different layers while masking others. Using different window sizes (individual layer, 2-layer, and 4-layer sliding windows), we observe that middle layers (12-20) contribute up to 7 percentage points more to model accuracy compared to the baseline (no mask, 0.436). This non-uniform sensitivity pattern across layers motivates LYNX’s dynamic approach to expert reduction, allowing aggressive pruning in less sensitive layers while preserving experts in critical layers.

We introduce two new policies in LYNX, with different objectives, namely latency preserving and accuracy preserving policy. These policies enable LYNX to reduce MoE inference latency with minimal cost to model accuracy by dynamically deciding which experts to retain for each layer.

4.2 Latency-preserving policy

Leveraging our key insight from Section 3.3 that dropping experts in prefill is lot more detrimental than dropping experts in decode, we implement an intelligent expert mapping policy called LYNX-Lat which maintains strict control over reduction in latency. In this policy, we extract the expert preferences for all tokens and perform voting to find the least frequently used experts for every incoming batch. If we encounter a decode batch, we drop a statically pre-determine number of experts for that layer while if it is prefill batch, we chose to retain all experts to ensure minimal loss to downstream accuracy.

While this policy ensures we always retain the most frequently used experts. We decide how many experts to drop and then drop the same fixed number of experts in each layer. Each expert within the $top - k$ experts is given the same weight and each token is given an equal vote. In order to better understand how much each layer contributes to the final output quality, we run an ablation study. For a given layer, we deny the first expert preference to each token of the batch, except for the layer we choose to mask. By creating a sliding window of masks, we analyse which layer contributes the most to accuracy when the token-to-expert mappings are preserved for that layer. In Figure 9, we observe that middle layers of the model seem to contribute significantly more to model accuracy compared to others. This non-uniform sensitivity to certain layers for a given model-task pair (Mixtral-8 \times 7B and GSM8k) emphasized the need for a dynamic policy which adaptively decided how many experts to drop in each layer.

4.3 Accuracy-preserving policy

Figure 10 shows LYNX’s architecture and highlights the accuracy preserving policy named LYNX-Acc. The system processes each incoming batch through carefully designed stages that determine expert computation. At the core, LYNX analyzes token importance and expert selection patterns to identify critical computations. These decisions are then refined based on the inference phase, enabling aggressive optimization during decode while preserving accuracy during prefill.

4.3.1 Token Importance Analysis

The foundation of LYNX’s design builds on our insight that router confidence predicts token sensitivity (Section 3.2). The system analyzes router logits to compute confidence scores for each token, using these scores to identify critical token-expert mappings that must be preserved. When batch sizes exceed our empirically determined threshold of 8 tokens, LYNX extracts a representative subset to maintain efficiency while preserving important patterns. This mechanism ensures that reduced expert computation still captures

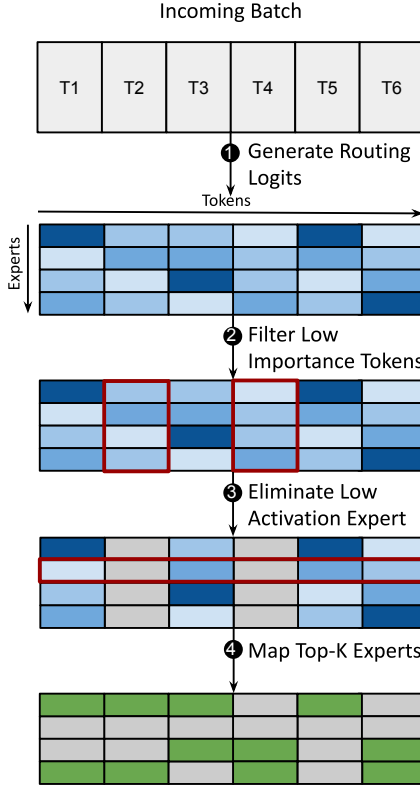


Figure 10: LYNX’s four-phase workflow for efficient MoE inference. Starting with an incoming token batch (T1-T6), the system: (1) generates routing logits to identify expert affinities, (2) filters out low-importance tokens based on router confidence scores (red boxes highlight filtered regions), (3) eliminates experts with low activation frequency across the remaining high-priority tokens, and (4) maps the final set of tokens to a reduced expert pool while preserving critical token-expert relationships. This dynamic workflow enables batch-level optimization of expert computation without requiring model modifications or offline tuning.

essential token-expert relationships.

4.3.2 Expert Selection Strategy

Building on our understanding of expert contribution hierarchy (Section 3.1), LYNX implements efficient expert selection with two operating modes. In accuracy-oriented operation, the system preserves primary expert assignments for high-confidence tokens while allowing more aggressive optimization for others. The latency-oriented mode maintains a fixed expert count per layer, optimizing for memory bandwidth while respecting critical token-expert mappings.

For tokens whose experts are dropped, LYNX implements intelligent remapping based on router logits, exploiting the high redundancy of secondary expert choices we observed in Section 3.1. This remapping ensures graceful degradation

when reducing expert computation.

4.3.3 Phase-specific Optimization

LYNX refines its token and expert decisions based on inference phase, exploiting the asymmetric sensitivity between prefill and decode (Section 3.3). During prefill, where computation is already well-parallelized and accuracy is critical, we maintain all expert assignments. For decode phases, where memory bandwidth dominates latency, we apply our token importance and expert selection strategies to reduce active experts.

This phase-aware approach directly addresses the tension between selective activation and batch serving identified in Section 2.2. By focusing optimization on decode, where memory bandwidth constraints are most severe, LYNX maintains efficiency without compromising the critical prefill computation.

4.4 Implementation Details

LYNX’s implementation focuses on minimizing overhead in the critical path of token generation. The system employs highly optimized torch libraries to perform runtime based expert selection for memory-bound decode, along with finding the optimal kernel dispatch parameters for different number of experts activated. Our implementation includes vectorized confidence score computation and sparse matrix operations designed specifically for reduced expert sets, with minimal synchronization requirements in the expert assignment path.

The system integrates with standard serving frameworks like vLLM (Kwon et al., 2023) through a lightweight runtime that intercepts and optimizes expert computation. This design allows immediate deployment without requiring model modifications or offline tuning.

5 EVALUATION

We evaluate LYNX across four tasks for variable number of experts retained during decode for Mixtral-8x7B-v0.1 (Table 2 and DBRX-Base (Table 1). We consider NAAE (Lu et al., 2024) as a baseline which also explores latency-accuracy trade-offs for MoE models. Our evaluation seeks to answer the following questions:

1. Can LYNX reduce the expert computation in the decode phase with minimal loss of accuracy on downstream tasks?
2. Does dynamically reducing the number of experts during decode phase with LYNX result in practical latency gains?
3. How does LYNX scale with batching for a given task?

Experts Retained	Method	Task			
		↑ HumanEval	↑ GSM8k	↑ TruthfulQA	↑ wmt16-en-to-de
4	LYNX-Acc *	34.14	62.62	46.14	29.21
	LYNX-Lat	31.10	28.66	33.29	4.98
8	LYNX-Acc *	36.23	72.55	49.20	33.78
	LYNX-Lat	37.56	63.23	29.62	19.73
12	LYNX-Acc *	39.43	73.16	48.59	34.85
	LYNX-Lat	37.80	68.23	35.37	31.98
16	Baseline All Experts	39.63	71.57	47.86	34.89

Table 1: DBRX performance across different tasks and retained experts. *For LYNX-Acc, the mean experts adaptively retained is ± 1 .

4. What is the impact of varying the threshold of token importance on the latency-accuracy trade-off made by LYNX?

Models and Environment: We evaluate LYNX across two MoE models namely, Mixtral-8 \times 7B (Jiang et al., 2024) and DBRX (Mosaic, 2024). These models are among the best open-source models in their model size categories. We use an A100-SXM4-80GB node which is equipped with four NVIDIA A100 GPUs, connected with all-to-all NVLINK. We run Mixtral 8x7B in a 2-way tensor-parallel configuration (TP-2), and DBRX Base in a 4-way tensor-parallel configuration (TP-4). We choose these configurations to ensure that we can fit the entire model in the GPU high bandwidth memory, which is crucial for latency-critical applications.

Workload: In order to measure the impact of our policies, we pick four generative tasks with reasonable decode lengths. GSM8k is a diverse grade school math word problems task which measures a model’s ability to solve multi-step mathematical reasoning problems (Cobbe et al., 2021). TruthfulQA is a test to measure model’s propensity to reproduce falsehoods commonly found online (Lin et al., 2021). HumanEval is a benchmark designed to evaluate an LLM’s code generation capabilities through hand-crafted programming challenges (Chen et al., 2021). The WMT16 English-to-German task focuses on evaluating model performance on machine translation (Bojar et al., 2016).

Metrics We report the per batch decode latency for various batch sizes and sequence lengths and number of experts for a given model. For accuracy, we pick the most appropriate metric as reported for ML tasks.

5.1 Accuracy Evaluation

We evaluate LYNX’s accuracy impact across two state-of-the-art MoE models: Mixtral-8 \times 7B and DBRX. Our evaluation reveals three key insights about dynamic expert reduction in production environments.

First, dynamic expert selection becomes increasingly critical for complex reasoning tasks. On GSM8k and HumanEval, which require multi-step reasoning and code generation respectively, LYNX’s LYNX-Acc policy maintains model capability even with significant expert reduction. When reducing Mixtral-8 \times 7B’s experts from eight to four, LYNX sees only a 4% accuracy drop on GSM8k, while the static baseline (NAEE) suffers a dramatic 20% degradation. This gap widens further with aggressive expert reduction - at two experts, LYNX maintains 43.97% accuracy on GSM8k while NAEE’s performance collapses to near-zero. These results suggest that dynamic expert selection is not just an optimization, but a requirement for maintaining model capability under resource constraints.

Second, our analysis reveals an intriguing pattern in task-specific robustness. Simpler tasks like machine translation (WMT16) and question-answering (TruthfulQA) demonstrate remarkable resilience to expert reduction. LYNX maintains baseline-equivalent accuracy while operating with just 50% of experts, suggesting these tasks rely on more redundant expert computation patterns. This insight opens possibilities for task-aware serving strategies that could dynamically adjust expert allocation based on workload characteristics.

Third, the benefits of dynamic expert selection scale with model size. For DBRX, with 16 experts per layer, LYNX’s runtime approach becomes particularly valuable. While static pruning faces combinatorial explosion (1820 possi-

Experts Retained	Method	Task			
		↑ HumanEval	↑ GSM8k	↑ TruthfulQA	↑ wmt16-en-to-de
2	LYNX-Acc *	23.17	43.97	47.37	16.92
	LYNX-Lat	19.51	42.23	45.17	19.44
	NAEE	0.0	14.78*	33.17	3.64
4	LYNX-Acc *	34.76	55.27	47.61	21.19
	LYNX-Lat	30.49	53.15	44.06	21.02
	NAEE	9.15	37.45*	47.37	20.04
6	LYNX-Acc *	38.41	58.61	45.90	22.31
	LYNX-Lat	35.37	56.71	44.06	22.15
	NAEE	28.04	50.87*	42.84	23.60
8	Baseline All Experts	37.80	59.14	45.17	22.46

Table 2: Mixtral performance across different tasks and retained experts. For NAEE on GSM8K, we report results obtained after pruning using the MATH calibration set. For all other tasks, we report results on the C4 calibration set. *For LYNX-Acc, the mean experts adaptively retained is ± 0.5 .

ble expert configurations per layer for 40 layers¹), LYNX’s LYNX-Acc policy maintains model quality with 25-50% expert reduction across all tasks. Most notably, on GSM8k, LYNX preserves baseline accuracy (71.57%) while running with just 8 experts, demonstrating that larger MoE models may contain significant computational redundancy that can be exploited at serving time.

Tables 2 and 1 detail these results across model configurations. All experiments use a decode batch size of 32, with LYNX’s LYNX-Lat policy targeting fixed expert ratios (25%, 50%, 75% of total experts) and the LYNX-Acc policy dynamically adjusting per-layer expert count to meet equivalent serving budgets. For the NAEE baseline, we use appropriate calibration datasets to prune experts, following the same reduction ratios as our LYNX-Lat policy. This comprehensive evaluation demonstrates that dynamic expert selection can effectively bridge the gap between MoE architecture efficiency and practical serving constraints.

5.2 Latency Evaluation

Understanding the latency characteristics of MoE models is crucial for production deployment. Unlike dense models where attention dominates computation time, MoE models present a different performance profile. Our analysis of Mixtral-8 \times 7B reveals that expert computation consumes approximately 83% of decode latency (Table 3), creating a significant optimization opportunity.

¹Due to the large number of configurations requiring evaluation for pruning, we do not evaluate NAEE with $e = 16$ for DBRX. Sampling approaches have been shown to result in collapse. (hao Liu et al., 2024)

BS	Attn	Route	MLP
8	1.54	0.06	7.07
16	3.03	0.07	14.03
32	5.15	0.07	27.91
64	11.34	0.09	55.86

Table 3: Computational cost breakdown (in milliseconds) across key MoE operations with varying batch sizes. Results show MLP computation and attention dominate inference time, while routing overhead remains negligible (<1%) across all batch sizes for sequence length 500, with Mixtral-8 \times 7B for four active experts.

The memory-bound nature of expert computation manifests in a direct relationship between latency and expert count. Figure 12 demonstrates this relationship across different serving configurations. LYNX achieves consistent latency improvements, with particularly strong results at moderate batch sizes (8-16) where speedups exceed 1.5 \times when reducing from eight to two experts. This performance gain holds remarkably stable across sequence lengths ranging from 500 to 2000 tokens.

Our rerouting system is extremely light-weight and is invoked at every layer for a given batch. It adds negligible latency overhead. From Table 3, we show that additional overhead introduced by our routing policy is negligible in comparison to the actual expert computation time, allowing us to fully materialize the latency speedup of dynamically reducing the number of experts.

Two key patterns emerge from our latency analysis. First, the relationship between expert reduction and speedup is non-linear. Reducing experts by half yields speedups be-

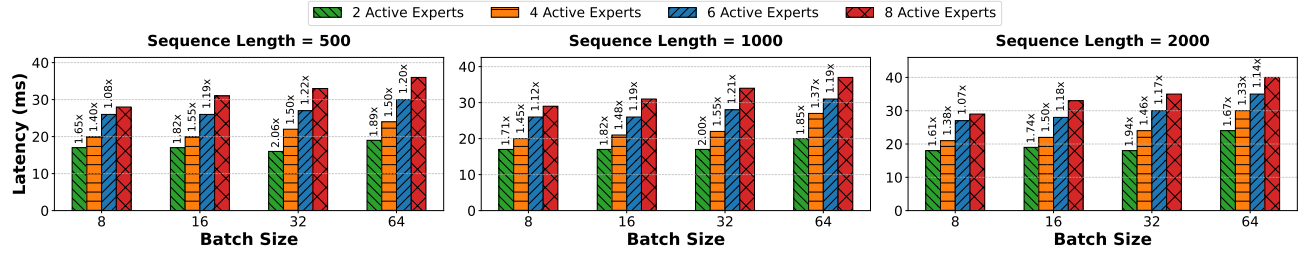


Figure 11: Latency speedup by reducing the total number of experts across batch sizes and sequence lengths for Mixtral

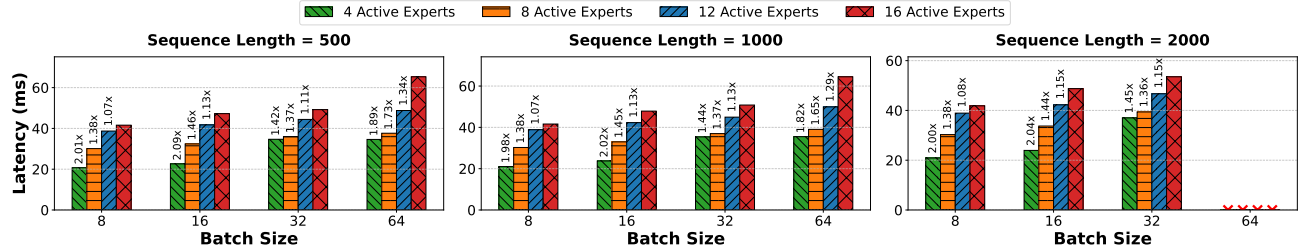


Figure 12: Latency speedup by reducing the total number of experts across batch sizes and sequence lengths for DBRX

tween $1.3\times$ to $1.5\times$, with diminishing returns for further reduction. This behavior stems from the growing relative cost of attention operations, which LYNX cannot optimize. Second, the efficacy of expert reduction varies with batch size and sequence length, suggesting opportunities for dynamic adaptation based on serving conditions.

The benefits of expert reduction scale with model size. For DBRX, with its larger expert pool (16 experts), the latency improvements become more pronounced. At batch size 64 and sequence length 500, reducing from sixteen to eight experts yields a $1.7\times$ speedup, extending to $1.9\times$ when further reducing to four experts. These results demonstrate that LYNX’s lightweight approach to expert reduction becomes increasingly valuable for larger models where memory bandwidth constraints are more severe.

These latency improvements come without requiring architectural changes, a priori workload knowledge or fine-tuning. Since MoE models are trained with a fixed $top-k$ activation pattern, LYNX only needs to ensure it maintains at least $top-k$ experts per layer while reducing the total expert pool. This constraint allows us to preserve the model’s fundamental operating characteristics while significantly improving serving performance.

¹GSM8K results for NAEE use prune-only configuration calibrated on MATH dataset, which provided the highest accuracy among tested configurations. NAEE calibrated using task-specific (MATH vs. C4) calibration sets as recommended by authors.

6 RELATED WORKS

Static Expert Pruning and Fine-tuning. Early approaches create reduced MoE variants through static pruning (Li et al., 2023) or expert merging based on similarity metrics. SEER-MoE (Muzio et al., 2024) extends this through sparsification and regularized fine-tuning, while others employ evolutionary search (hao Liu et al., 2024) for expert reduction. However, these methods require task-specific calibration and additional training overhead.

Dynamic Expert Management. Recent work (Lu et al., 2024) explores dynamic runtime expert activation based on workload characteristics by varying $top - k$ across batches. However, these approaches struggle with batch serving where activation patterns inevitably result in full expert utilization. Additionally, the approach requires offline calibration on a representative dataset.

Model Compression. Traditional compression techniques adapt pruning and quantization for MoEs (He et al., 2024). FP16/FP8 quantization (Xiao et al., 2023; Lin et al., 2024) can reduce memory footprint by 50-75%, at the expense of accuracy trade-offs. LYNX complements these approaches for latency-sensitive deployments.

Expert Placement and Execution. Several systems focus on efficient expert distribution across devices. GShard (Lepikhin et al., 2020) introduces expert parallelism, while recent work (Huang et al., 2023) optimizes communication through dynamic gating. Systems like (Chen et al., 2022) explore predictive expert pre-fetching, enabling CPU-GPU expert

management (Xue et al., 2024; Eliseev & Mazur, 2023). Fiddler (Kamahori et al., 2024) and MoESys (Fedus et al., 2022) optimize expert placement for resource-constrained environments. LYNX’s approach is complementary to these system-level optimizations.

7 CONCLUSION

The Mixture-of-Experts architecture and request batching improve the efficiency of ML inference at scale. Interestingly, this paper shows that use of batching diminishes the efficiency gains expected from MoE models. We demonstrate improvement upon fixed and ahead-of-time expert selection approaches used in prior work. We develop LYNX, a new system that performs dynamic expert selection at batch granularity across layers without any workload knowledge a priori. Using two different models of varying sizes and several representative downstream tasks, we show that LYNX opens up a new trade-off in inference performance, affording nearly $1.5\times$ speedup with minimal drop in accuracy compared to prior work using the same amount of resources.

REFERENCES

Agrawal, A., Kedia, N., Panwar, A., Mohan, J., Kwatra, N., Gulavani, B. S., Tumanov, A., and Ramjee, R. Taming throughput-latency tradeoff in llm inference with sarathi-serve. *ArXiv*, abs/2403.02310, 2024. URL <https://api.semanticscholar.org/CorpusID:268249103>.

Anthropic. Claude, 2024. URL <https://claude.ai/>. Accessed: 2024-10-31.

Bojar, O., Chatterjee, R., Federmann, C., Graham, Y., Hadidow, B., Huck, M., Jimeno-Yepes, A., Koehn, P., Logacheva, V., Monz, C., Negri, M., Névéol, A., Neves, M., Popel, M., Post, M., Rubino, R., Scarton, C., Specia, L., Turchi, M., Verspoor, K. M., and Zampieri, M. Findings of the 2016 conference on machine translation. In *Conference on Machine Translation*, 2016. URL <https://api.semanticscholar.org/CorpusID:14421595>.

Chen, M., Tworek, J., Jun, H., Yuan, Q., Pondé, H., Kaplan, J., Edwards, H., Burda, Y., Joseph, N., Brockman, G., Ray, A., Puri, R., Krueger, G., Petrov, M., Khlaaf, H., Sastry, G., Mishkin, P., Chan, B., Gray, S., Ryder, N., Pavlov, M., Power, A., Kaiser, L., Bavarian, M., Winter, C., Tillet, P., Such, F. P., Cummings, D. W., Plappert, M., Chantzis, F., Barnes, E., Herbert-Voss, A., Guss, W. H., Nichol, A., Babuschkin, I., Balaji, S., Jain, S., Carr, A., Leike, J., Achiam, J., Misra, V., Morikawa, E., Radford, A., Knight, M. M., Brundage, M., Murati, M., Mayer, K., Welinder, P., McGrew, B., Amodei, D., McCandlish, S., Sutskever, I., and Zaremba, W. Evaluating large language models trained on code. *ArXiv*, abs/2107.03374, 2021. URL <https://api.semanticscholar.org/CorpusID:235755472>.

Chen, T., Huang, S., Xie, Y., Jiao, B., Jiang, D., Zhou, H., Li, J., and Wei, F. Task-specific expert pruning for sparse mixture-of-experts. *ArXiv*, abs/2206.00277, 2022. URL <https://api.semanticscholar.org/CorpusID:249240535>.

Chen, T., Zhang, Z. A., Jaiswal, A., Liu, S., and Wang, Z. Sparse moe as the new dropout: Scaling dense and self-slimmable transformers. *ArXiv*, abs/2303.01610, 2023. URL <https://api.semanticscholar.org/CorpusID:257353502>.

Cobbe, K., Kosaraju, V., Bavarian, M., Chen, M., Jun, H., Kaiser, L., Plappert, M., Tworek, J., Hilton, J., Nakano, R., Hesse, C., and Schulman, J. Training verifiers to solve math word problems. *ArXiv*, abs/2110.14168, 2021. URL <https://api.semanticscholar.org/CorpusID:239998651>.

Do, G., Khiem, L., Pham, Q. H., Nguyen, T., Doan, T.-N., Nguyen, B., Liu, C., Ramasamy, S., Li, X., and Hoi, S. C. H. Hyperrouter: Towards efficient training and inference of sparse mixture of experts. *ArXiv*, abs/2312.07035, 2023. URL <https://api.semanticscholar.org/CorpusID:266163896>.

Eliseev, A. and Mazur, D. Fast inference of mixture-of-experts language models with offloading. *ArXiv*, abs/2312.17238, 2023. URL <https://api.semanticscholar.org/CorpusID:266573098>.

Fedus, W., Zoph, B., and Shazeer, N. Switch transformers: scaling to trillion parameter models with simple and efficient sparsity. *J. Mach. Learn. Res.*, 23(1), jan 2022. ISSN 1532-4435.

hao Liu, E., Zhu, J., Lin, Z., Ning, X., Blaschko, M. B., Yan, S., Dai, G., Yang, H., and Wang, Y. Efficient expert pruning for sparse mixture-of-experts language models: Enhancing performance and reducing inference costs. 2024. URL <https://api.semanticscholar.org/CorpusID:270869609>.

He, S., Dong, D., Ding, L., and Li, A. Demystifying the compression of mixture-of-experts through a unified framework, 2024. URL <https://arxiv.org/abs/2406.02500>.

Huang, H., Ardalani, N., Sun, A., Ke, L., Lee, H.-H. S., Sridhar, A., Bhosale, S., Wu, C.-J., and Lee, B. Towards

moe deployment: Mitigating inefficiencies in mixture-of-expert (moe) inference. *ArXiv*, abs/2303.06182, 2023. URL <https://api.semanticscholar.org/CorpusID:257496628>.

Jiang, A. Q., Sablayrolles, A., Roux, A., Mensch, A., Savary, B., Bamford, C., Chaplot, D. S., de Las Casas, D., Hanna, E. B., Bressand, F., Lengyel, G., Bour, G., Lample, G., Lavaud, L. R., Saulnier, L., Lachaux, M.-A., Stock, P., Subramanian, S., Yang, S., Antoniak, S., Scao, T. L., Gervet, T., Lavril, T., Wang, T., Lacroix, T., and Sayed, W. E. Mixtral of experts. *ArXiv*, abs/2401.04088, 2024. URL <https://api.semanticscholar.org/CorpusID:266844877>.

Kamahori, K., Gu, Y., Zhu, K., and Kasikci, B. Fidler: Cpu-gpu orchestration for fast inference of mixture-of-experts models. *ArXiv*, abs/2402.07033, 2024. URL <https://api.semanticscholar.org/CorpusID:267627732>.

Kaplan, J., McCandlish, S., Henighan, T., Brown, T. B., Chess, B., Child, R., Gray, S., Radford, A., Wu, J., and Amodei, D. Scaling laws for neural language models. *ArXiv*, abs/2001.08361, 2020. URL <https://api.semanticscholar.org/CorpusID:210861095>.

Kwon, W., Li, Z., Zhuang, S., Sheng, Y., Zheng, L., Yu, C. H., Gonzalez, J. E., Zhang, H., and Stoica, I. Efficient memory management for large language model serving with pagedattention. In *Proceedings of the ACM SIGOPS 29th Symposium on Operating Systems Principles*, 2023.

Lepikhin, D., Lee, H., Xu, Y., Chen, D., Firat, O., Huang, Y., Krikun, M., Shazeer, N. M., and Chen, Z. Gshard: Scaling giant models with conditional computation and automatic sharding. *ArXiv*, abs/2006.16668, 2020. URL <https://api.semanticscholar.org/CorpusID:220265858>.

Li, P., Zhang, Z. A., Yadav, P., Sung, Y.-L., Cheng, Y., Bansal, M., and Chen, T. Merge, then compress: Demystify efficient smoe with hints from its routing policy. *ArXiv*, abs/2310.01334, 2023. URL <https://api.semanticscholar.org/CorpusID:263605809>.

Lin, J., Tang, J., Tang, H., Yang, S., Chen, W.-M., Wang, W.-C., Xiao, G., Dang, X., Gan, C., and Han, S. Awq: Activation-aware weight quantization for llm compression and acceleration. In *MLSys*, 2024.

Lin, S. C., Hilton, J., and Evans, O. Truthfulqa: Measuring how models mimic human falsehoods. In *Annual Meeting of the Association for Computational Linguistics*, 2021. URL <https://api.semanticscholar.org/CorpusID:237532606>.

Lu, X., Liu, Q., Xu, Y., Zhou, A., Huang, S., Zhang, B., Yan, J., and Li, H. Not all experts are equal: Efficient expert pruning and skipping for mixture-of-experts large language models. *ArXiv*, abs/2402.14800, 2024. URL <https://api.semanticscholar.org/CorpusID:267782440>.

Luo, X., Rechardt, A., Sun, G., Nejad, K. K., Y'a~nez, F., Yilmaz, B., Lee, K., Cohen, A. O., Borghesani, V., Pashkov, A., Marinazzo, D., Nicholas, J., Salatiello, A., Sucholutsky, I., Minervini, P., Razavi, S., Rocca, R., Yusifov, E., Okalova, T., Gu, N., Ferianc, M., Khona, M., Patil, K. R., Lee, P.-S., Mata, R., Myers, N. E., Bizley, J. K., Musslick, S., Bilgin, I. P., Niso, G., Ales, J. M., Gaebler, M., Murty, A. R., Hall, C. M., Dafflon, J., Bao, S. D., and Love, B. C. Large language models surpass human experts in predicting neuroscience results. *ArXiv*, abs/2403.03230, 2024. URL <https://api.semanticscholar.org/CorpusID:268253470>.

Mosaic. Introducing dbrx: A new state-of-the-art open llm, March 2024. URL <https://www.databricks.com/blog/introducing-dbrx-new-state-art-open-llm>. Accessed: 2024-10-30.

Muzio, A., Sun, A., and He, C. Seer-moe: Sparse expert efficiency through regularization for mixture-of-experts. *ArXiv*, abs/2404.05089, 2024. URL <https://api.semanticscholar.org/CorpusID:269005367>.

Naveed, H., Khan, A. U., Qiu, S., Saqib, M., Anwar, S., Usman, M., Barnes, N., and Mian, A. S. A comprehensive overview of large language models. *ArXiv*, abs/2307.06435, 2023. URL <https://api.semanticscholar.org/CorpusID:259847443>.

OpenAI. Chatgpt, 2024. URL <https://www.openai.com/chatgpt>. Accessed: 2024-10-31.

Xiao, G., Lin, J., Seznec, M., Wu, H., Demouth, J., and Han, S. SmoothQuant: Accurate and efficient post-training quantization for large language models. In *Proceedings of the 40th International Conference on Machine Learning*, 2023.

Xue, L., Fu, Y., Lu, Z., Mai, L., and Marina, M. Moe-infinity: Activation-aware expert offloading for efficient moe serving. *ArXiv*, abs/2401.14361, 2024. URL <https://api.semanticscholar.org/CorpusID:267211688>.

Yin, Z., Sun, Q., Guo, Q., Zeng, Z., Li, X., Sun, T., Chang, C., Cheng, Q., Wang, D., Mou, X.,

Qiu, X., and Huang, X. Aggregation of reasoning: A hierarchical framework for enhancing answer selection in large language models. In *International Conference on Language Resources and Evaluation*, 2024. URL <https://api.semanticscholar.org/CorpusID:269804400>.

Yu, G.-I. and Jeong, J. S. Orca: A distributed serving system for transformer-based generative models. In *USENIX Symposium on Operating Systems Design and Implementation*, 2022. URL <https://api.semanticscholar.org/CorpusID:251734964>.

Yun, L., Zhuang, Y., Fu, Y., Xing, E. P., and Zhang, H. Toward inference-optimal mixture-of-expert large language models. *ArXiv*, abs/2404.02852, 2024. URL <https://api.semanticscholar.org/CorpusID:268875826>.